blood®
Regular Article

HEMATOPOIESIS AND STEM CELLS

Regulation of lymphoid-myeloid lineage bias through regnase-1/3-mediated control of Nfkbiz

Takuya Uehata,[1,*] Shinnosuke Yamada,[1,*] Daisuke Ori,[1] Alexis Vandenbon,[2] Amir Giladi,[3] Adam Jelinski,[3] Yasuhiro Murakawa,[4] Hitomi Watanabe,[5] Kazuhiro Takeuchi,[4] Kazunori Toratani,[1] Takashi Mino,[1] Hisanori Kiryu,[6] Daron M. Standley,[7] Tohru Tsujimura,[8] Tomokatsu Ikawa,[9] Gen Kondoh,[5] Markus Landthaler,[10] Hiroshi Kawamoto,[11] Hans-Reimer Rodewald,[12] Ido Amit,[3] Ryo Yamamoto,[4] Masaki Miyazaki,[11] and Osamu Takeuchi[1]

[1]Department of Medical Chemistry, Graduate School of Medicine, and [2]Laboratory of Tissue Homeostasis, Institute for Life and Medical Sciences, Kyoto University, Kyoto, Japan; [3]Department of Immunology, Weizmann Institute of Science, Rehovot, Israel; [4]Institute for the Advanced Study of Human Biology and [5]Laboratory of Integrative Biological Sciences, Institute for Life and Medical Sciences, Kyoto University, Kyoto, Japan; [6]Department of Computational Biology and Medical Sciences, Graduate School of Frontier Sciences, The University of Tokyo, Chiba, Japan; [7]Department of Genome Informatics, Genome Information Research Center, Research Institute for Microbial Diseases, Osaka University, Osaka, Japan; [8]Department of Pathology, Hyogo College of Medicine, Hyogo, Japan; [9]Division of Immunology and Allergy, Research Institute for Biomedical Sciences, Tokyo University of Science, Chiba, Japan; [10]RNA Biology and Posttranscriptional Regulation, Max Delbrück Center for Molecular Medicine Berlin, Berlin Institute for Molecular Systems Biology, Berlin, Germany; [11]Laboratory of Immunology, Institute for Life and Medical Sciences, Kyoto University, Kyoto, Japan; and [12]Division for Cellular Immunology, German Cancer Research Center, Heidelberg, Germany

KEY POINTS

- **Reg1 and Reg3 are ribonucleases critical for determining lymphoid fate and restricting myeloid differentiation in HSPCs.**
- **Reg1/Reg3-mediated decay of *Nfkbiz*, crucial for HSPC lineage choice, is potently manipulated by an antisense oligonucleotide.**

Regulation of lineage biases in hematopoietic stem and progenitor cells (HSPCs) is pivotal for balanced hematopoietic output. However, little is known about the mechanism behind lineage choice in HSPCs. Here, we show that messenger RNA (mRNA) decay factors regnase-1 (Reg1; Zc3h12a) and regnase-3 (Reg3; Zc3h12c) are essential for determining lymphoid fate and restricting myeloid differentiation in HSPCs. Loss of *Reg1* and *Reg3* resulted in severe impairment of lymphopoiesis and a mild increase in myelopoiesis in the bone marrow. Single-cell RNA sequencing analysis revealed that Reg1 and Reg3 regulate lineage directions in HSPCs via the control of a set of myeloid-related genes. Reg1- and Reg3-mediated control of mRNA encoding *Nfkbiz*, a transcriptional and epigenetic regulator, was essential for balancing lymphoid/myeloid lineage output in HSPCs in vivo. Furthermore, single-cell assay for transposase-accessible chromatin sequencing analysis revealed that Reg1 and Reg3 control the epigenetic landscape on myeloid-related gene loci in early stage HSPCs via *Nfkbiz*. Consistently, an antisense oligonucleotide designed to inhibit Reg1- and Reg3-mediated *Nfkbiz* mRNA degradation primed hematopoietic stem cells toward myeloid lineages by enhancing *Nfkbiz* expression. Collectively, the collaboration between posttranscriptional control and chromatin remodeling by the Reg1/Reg3-*Nfkbiz* axis governs HSPC lineage biases, ultimately dictating the fate of lymphoid vs myeloid differentiation.

Introduction

Hematopoietic stem and progenitor cells (HSPCs) in the bone marrow (BM) generate multilineages that contribute to the production of all mature blood and immune cells. This process is tightly controlled to maintain the balance between lymphoid, myeloid, erythroid, and megakaryocytic cell populations under steady state conditions.[1-3] Consistent with the recent lineage-biased output model of HSPCs,[4-7] the pattern of gene expression in the progenitor reflects that of the mature cell type toward which it is biased, a phenomenon known as transcriptional lineage priming.[1,8,9] This is initiated by cell-intrinsic and -extrinsic factors controlling lineage-determining transcription programs. Under microbial infection, inflammatory cytokines such as interleukin-1β (IL-1β) and tumor necrosis factor (TNF) trigger reprograming of transcriptional networks in HSPCs to prime myelopoiesis by inducing the lineage-determining transcription factors (TFs) PU.1 and C/EBPβ.[10-17] In addition, alterations in epigenetic landscape can contribute to transcriptional lineage priming in a cell-intrinsic manner.[18-20] However, molecular mechanisms that explain the link between lineage output and transcriptional status need to be clarified.

Regnase-1 (Reg1) is an endoribonuclease that degrades messenger RNAs (mRNAs) harboring stem-loop (SL) structures with a pyrimidine-purine-pyrimidine loop in the 3′ untranslated regions (UTRs).[21-23] Reg1 is critical for the suppression of inflammatory responses in mature immune cells and for the

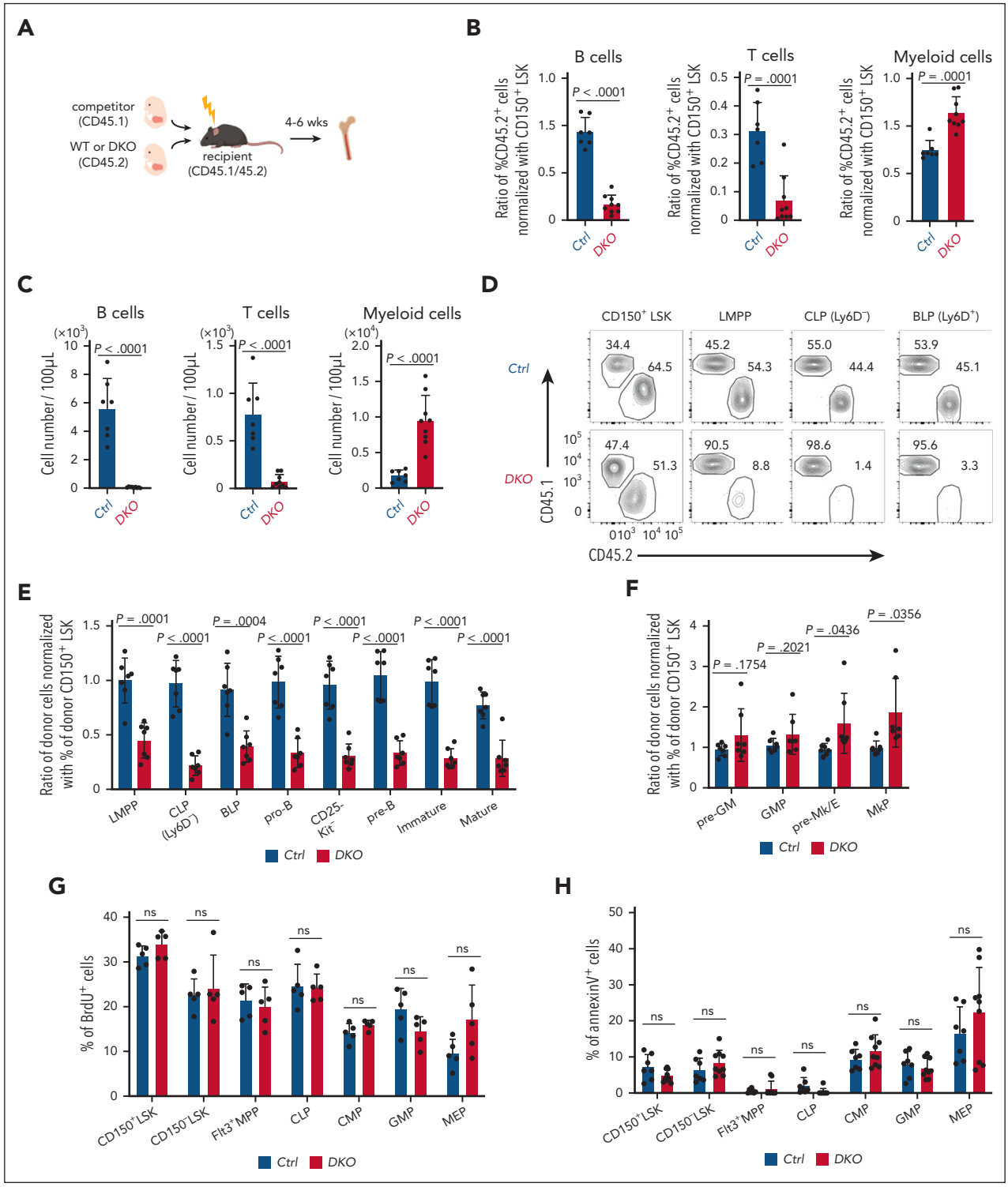

Figure 1. Reg1 and Reg3 are essential for early stage lymphopoiesis in a cell-intrinsic manner. (A-F) Competitive FL transplantation. (A) Experimental workflow of competitive transplantation using FL cells (E15.5). (B-C) Relative frequencies and cell numbers of donor immune cells in the peripheral blood. (B) Each dot represents the ratio of the percentage of CD45.2 in each population to the percentage of CD45.2 in SLAM$^+$ Lin$^-$Sca1$^+$Kit$^+$ (LSK) from recipient mice. Donor B cells, T cells, and myeloid cells were defined as CD45.2$^+$ B220$^+$CD19$^+$ cells, CD4/8$^+$TCRβ$^+$ cells, and CD11b$^+$ cells, respectively. (D) Representative flow cytometric plots of CD45.1 and CD45.2 expression gated on CD150$^+$ LSK, LMPP (Flt3^{hi}LSK), CLP (Ly6D$^-$Flt3$^+$IL-7Rα$^+$Sca1^{dull}Kit^{dull}), and BLP (Ly6D$^+$Flt3$^+$IL-7Rα$^+$Sca1^{dull}Kit^{dull}). Numbers in plots indicate the percentage of CD45.1$^+$ or CD45.2$^+$ cells. (E-F) Relative frequencies of each population in the BM. Each dot represents the ratio of the percentage of CD45.2 in each population to the percentage of CD45.2 in CD150$^+$ LSK from recipient mice. (G-H) in vivo BrdU incorporation and annexin V staining in CD150$^+$ LSK, CD150$^-$ LSK, Flt3$^+$ MPP, CLP, CMP, GMP, and MEP in the BM of mice competitively transplanted with FL cells, as in panel A. (E-F) Data are a composite of 3 independent experiments. (G-H) Data are representative from 3 independent experiments. Data are presented as mean ± standard deviation (SD) (B-C,E-H). Statistical significance was calculated by unpaired 2-tailed Student *t* test (B-C,E-H). BrdU, Bromodeoxyuridine; BLP, B-cell-biased lymphoid progenitor; CLP, common lymphoid progenitor; CMP, granulocyte-monocyte progenitor; GMP, granulocyte-monocyte progenitor; MEP, megakaryocyte–erythroid progenitor; LMPP, lymphoid primed multipotent progenitor; ns, not significant.

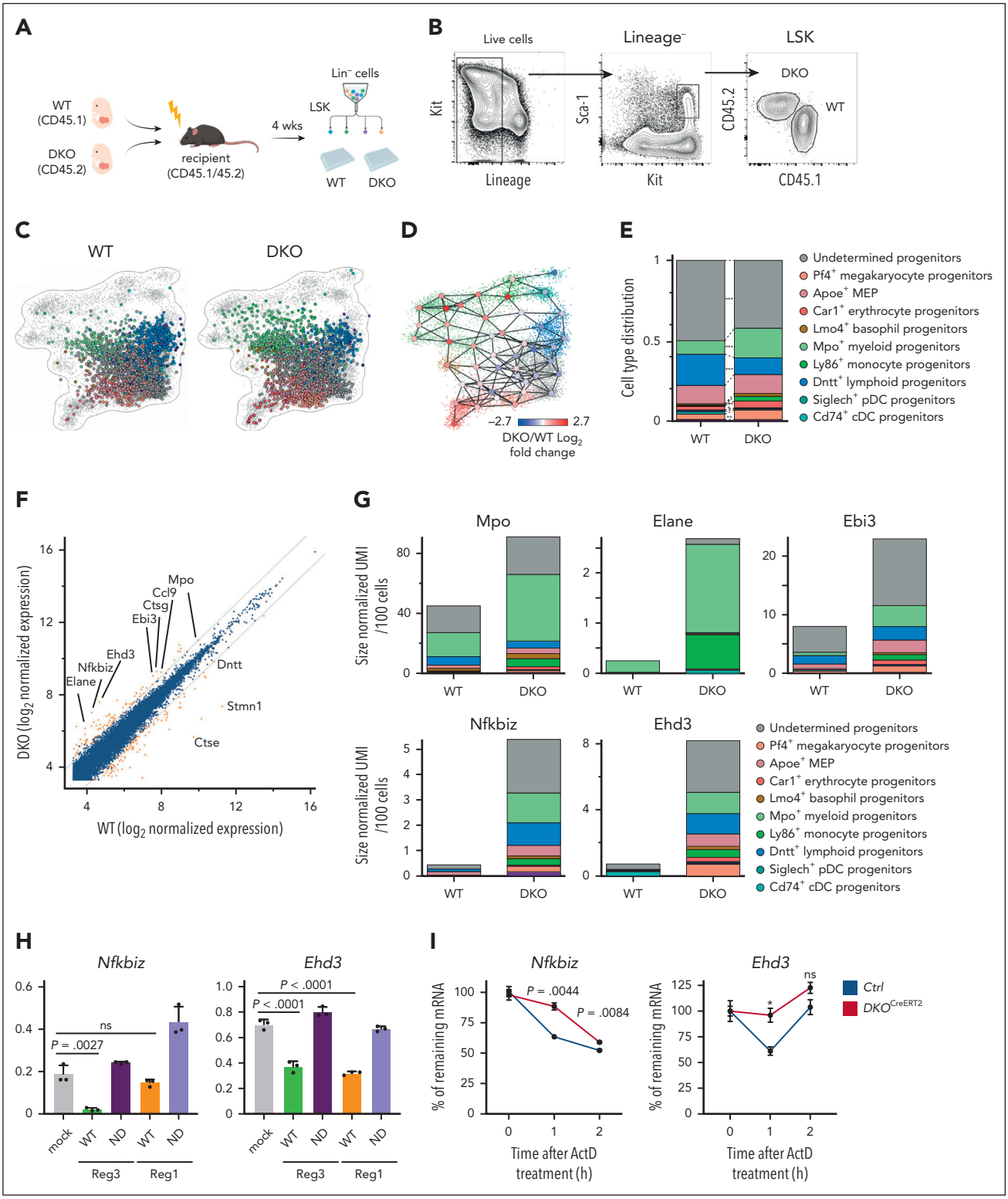

Figure 2. Reg1 and Reg3 control lineage biases within HSPCs. (A) Schematic representation of experimental strategy for single-cell sorting. (B) Gating strategy for WT and *Reg1*$^{-/-}$*Reg3*$^{-/-}$ (DKO) LSK cells sorted from the identical mouse receiving WT (CD45.1) and DKO (CD45.2) FL cells. (C) A 2-dimensional projection of 2241 single cells sorted from WT (CD45.1) LSK and 2242 single cells from DKO (CD45.2) LSK onto the reference model. Cells are colored according to assignment to reference model meta cells (see "Methods"). (D) Difference in meta-cell abundance between single cells sorted from DKO and WT mice. Each circle represents a reference meta cell. Circle color represents $\log_2$ (fold change) in meta-cell abundance between the 2 genetic backgrounds. (E) Cell type distribution of single cells sorted from WT and DKO mice. *$P < .05$; **$P < .001$; ***$P < .00001$. (F) Differential gene expression between pooled cells from DKO cells compared with WT cells. Gold dots indicate differentially expressed genes (FDR corrected $P < .001$ under χ^2 test) with fold change >2. Diagonal lines show $\log_2$ (fold change) = −1 or 1. Values represent $\log_2$ size–normalized expression. (G) Total expression of specific genes in different genetic backgrounds. Values represent size-normalized total transcripts per 100 cells. Colors represent relative contribution from the different hematopoietic core subsets. (H) Luciferase activity was assessed by using pGL3 plasmids containing the 3′ UTR of *Nfkbiz* and *Ehd3*, together with mock or plasmids for WT or nuclease-dead mutant for Reg1 and Reg3 (n = 3 each). Data are representative of at least 3 independent experiments. (I) mRNA stability of *Nfkbiz* and *Ehd3* in Lin⁻ cells from

maintenance of immune homeostasis.[24,25] There are 4 regnase family members (Reg1 to Reg4) in mammals characterized by the presence of a ribonuclease (RNase) domain and a CCCH-type zinc finger (Zf) domain. However, it remains unclear to what extent the regnase family members play redundant roles in the immune system.

In this study, we clarified the roles of Reg1 and Reg3 in HSPC lineage choice through the control of *Nfkbiz* mRNA stability. Further, we developed a method that induces hematopoietic stem cell (HSC) myeloid priming by using an antisense oligonucleotide (ASO) that inhibits Reg1/Reg3-mediated *Nfkbiz* degradation.

Methods

scRNA-seq

Single-cell sorting for single-cell RNA sequencing (scRNA-seq) was performed as previously described.[26,27] Briefly, lineage-negative (Lin^-) cells were purified from mice competitively reconstituted with wild type (WT; CD45.1) and *Reg1/Reg3*-deficient (*DKO*; CD45.2) fetal liver (FL) cells. WT and *DKO* $Lin^-Sca1^+Kit^+$ (LSK) cells were sc-sorted into 384-well cell capture plates containing lysis solution and barcoded poly(T) reverse-transcription (RT) primers. Immediately after sorting, each plate was spun down to ensure cell immersion into the lysis solution, snap frozen on dry ice, and stored at −80°C until processed.

Full details are provided in the supplemental Methods (available on the *Blood* website).

Results

Reg1 and Reg3 are essential for balanced lineage output in BM

Among regnase family members, Lin^- hematopoietic progenitor highly express Reg1 and Reg3 (supplemental Figure 1A-C). Therefore, we investigated whether Reg1 and Reg3 regulate hematopoietic differentiation in the BM. Because mice lacking both *Reg1* and *Reg3* (*DKO*) but not *Reg1* or *Reg3* alone (supplemental Figure 1C-E) exhibited perinatal lethality, accompanied by marked infiltration of neutrophils in the periportal region of the liver and the parenchyma of the pancreas (supplemental Figure 1F). To investigate hematopoiesis, we performed fetal liver (FL) transplantation using E15.5 fetuses of $Reg1^{-/-}$, $Reg3^{-/-}$, or *DKO* donors and euthanized them 4 to 6 weeks after transplantation. Interestingly, *DKO* FL-transplanted mice displayed a profound loss of $B220^+CD19^+$ B cells and a reciprocal increase in $CD11b^+$ myeloid cells in the peripheral blood compared with control (supplemental Figure 1G-H). In contrast, deficiency of *Reg1* or *Reg3* alone did not lead to profound changes in immune cells. Consistently, E15.5 *DKO* FL cells exhibited decreased B cells and increased myeloid cells (supplemental Figure 1I). These results suggest the redundant roles of Reg1 and Reg3 in hematopoiesis.

To investigate whether the influence of *Reg1/Reg3* deficiency on BM hematopoiesis is cell-intrinsic, we performed competitive FL transplants. We engrafted equal numbers of control or *DKO* FL cells (CD45.2) alongside competitor cells (CD45.1) into lethally irradiated recipient mice (CD45.1/45.2) (Figure 1A). We observed comparable engraftment levels in mice receiving control and *DKO* FL cells (supplemental Figure 2A). *DKO* FL–transplanted mice showed a significant reduction of B/T-lymphocytes and a concomitant increase in myeloid cells in the peripheral blood in frequencies and numbers (Figure 1B-C). A similar trend was observed in the BM, marked by reduced B-cell numbers and an increase in $Gr\text{-}1^+CD11b^+$ myeloid cells (supplemental Figure 2B-C). Consistently, thymic T cell populations were reduced in *DKO* mice compared with that of controls (supplemental Figure 2D). The analysis of BM hematopoietic progenitors in mixed chimera revealed that *DKO* cells failed to give rise to all B cell lineage cells and showed unimpaired or mildly increased proportion of megakaryocytic-erythroid and myeloid lineages (Figure 1D-F).

We then asked whether Reg1 and Reg3 were required for B-lymphopoiesis in uncommitted or lymphoid lineage-committed progenitor stages. To address this, we used *Il7r*-cre^+ROSA-yellow fluorescent protein $(YFP)^+Reg1^{fl/fl}Reg3^{-/-}$ mice ($DKO^{Il7r\text{-}cre}$), in which *Reg1* gene was deleted via *Il7r*-driven cre recombination. We confirmed *Il7r*-cre–mediated recombination at the pro-B stage and, to a lesser extent, the common lymphoid progenitor (CLP) based on RT polymerase chain reaction (RT-PCR) for *Reg1* and YFP expression (supplemental Figure 2E-F). Through competitive FL transplantation experiments, we observed that B-cell differentiation remained unchanged in YFP-expressing $DKO^{Il7r\text{-}cre}$ cells compared with their control counterparts (supplemental Figure 2G). These results indicate that Reg1 and Reg3 function at uncommitted stages of B-lymphopoiesis and become dispensable once the cells undergo lineage commitment.

To understand how Reg1 and Reg3 regulate BM hematopoiesis, we examined the proliferative activity and cell viability of uncommitted progenitors. In vivo bromodeoxyuridine (BrdU) incorporation experiments using mixed chimera receiving control and *DKO* FL cells showed no difference in proliferative activity of $CD150^+$ or $CD150^-$ LSK, $Flt3^+$ multipotent progenitor (MPP), CLP, or myeloid progenitors such as common myeloid progenitor (CMP), granulocyte-monocyte progenitor (GMP), and megakaryocyte–erythroid progenitor (MEP) between these genotypes (Figure 1G). In addition, annexin V–positive apoptotic cell frequencies were comparable between the control and *DKO* (Figure 1H). These results suggest that Reg1 and Reg3 regulate lymphoid lineage differentiation, rather than affecting cell proliferation or viability.

To evaluate the roles of Reg1 and Reg3 in steady-state hematopoiesis, we generated *Reg1* conditional knockout mice crossed with $Reg3^{-/-}$ animals, using tamoxifen-inducible cre recombinase system (supplemental Figure 3A-B). $CreERT2^+Reg1^{fl/fl}Reg3^{-/-}$ ($DKO^{CreERT2}$) mice also exhibited a reduction in $B220^+CD19^+$ B cells and an increase in $CD11b^+$ myeloid cells both in frequencies and numbers, at day 14 after tamoxifen injection (supplemental Figure 3C-D). We next examined HSPC subpopulations

Figure 2 (continued) control and $DKO^{CreERT2}$ mice. Cells were stimulated with IL-1β for 2 hours, followed by addition of actinomycin D (ActD). The remaining transcripts relative to the 0-hour time point were measured by quantitative RT-PCR. Data are representative of 2 independent experiments (H-I). Data are presented as mean ± SD (H) or ± standard error of the mean (I). Statistical significance was calculated by 2-tailed Fisher exact test (E), 1-way analysis of variance (ANOVA) with Holm-Sidak multiple comparisons test (H), or unpaired 2-tailed Student *t* test (I). ND, nuclease dead.

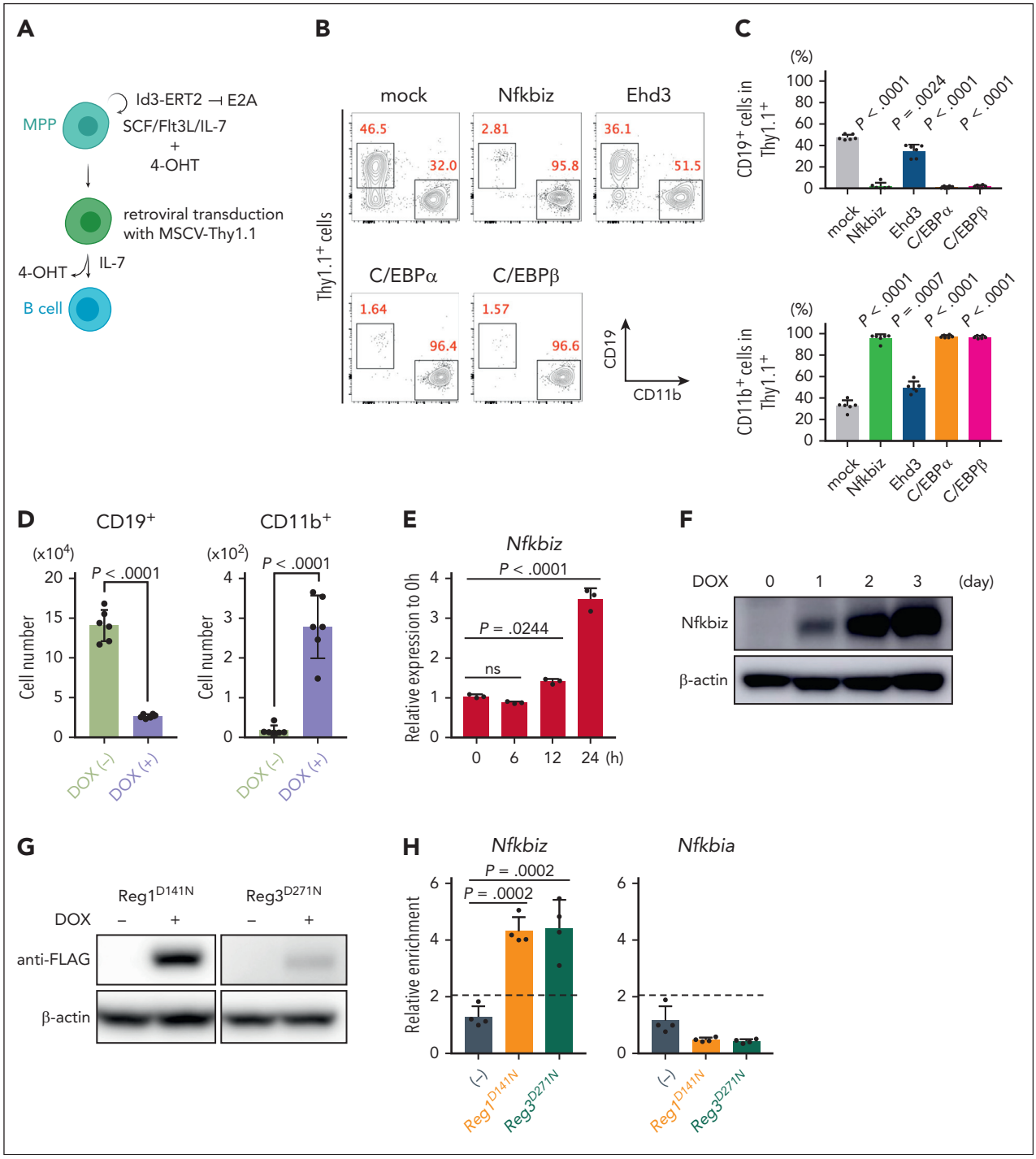

Figure 3. Nfkbiz is a direct target gene for Reg1 and Reg3 that is potent to promote myelopoiesis. (A) Schematic representation for B-cell differentiation of multipotent progenitor (MPP$^{Hid3\text{-}ERT2}$) cells retrovirally transduced with MSCV-Thy1.1 vector. Cells were then cultured under B-cell–differentiation condition. (B-C) In vitro B-cell differentiation in MPP$^{Hid3\text{-}ERT2}$ cells retrovirally overexpressing Nfkbiz and Ehd3 as well as myeloid-lineage TFs. At day 7, cells were analyzed by flow cytometry. Flow cytometry plots of CD19 and CD11b after gated on Thy1.1$^+$ cells (B) and percentages of CD19$^+$ and CD11b$^+$ Thy1.1$^+$ cells (C) were shown (n = 6 each). (D) Numbers of CD19$^+$CD11b$^-$ and CD19$^-$CD11b$^+$ cells in tetO-*cre-Reg1*$^{fl/fl}$*Reg3*$^{-/-}$ MPP$^{Hid3\text{-}ERT2}$ cells cultured under B-cell–differentiating condition in the presence or absence of DOX at day 6 (n = 6 each). (E-F) Quantitative RT-PCR (E) and immunoblot analysis (F) of *Nfkbiz* in tetO-*cre-Reg1*$^{fl/fl}$*Reg3*$^{-/-}$ MPP$^{Hid3\text{-}ERT2}$ cells at the indicated time points after DOX treatment (n = 3 each in E). Cells were cultured under stem-cell condition for the indicated time. (G) DOX-inducible overexpression of FLAG-tagged Reg1 (D141N) or Reg3 (D271N) in tetO-*cre-Reg1*$^{fl/fl}$*Reg3*$^{-/-}$ MPP$^{Hid3\text{-}ERT2}$ cells. (H) RNA immunoprecipitation quantitative PCR (RIP-qPCR) analysis of a set of genes from lysates of tetO-*cre-Reg1*$^{fl/fl}$*Reg3*$^{-/-}$ MPP$^{Hid3\text{-}ERT2}$ cells expressing FLAG-tagged Reg1 or Reg3 as in (G) (n = 4 each). Data are representative of 2 (B-D, G-H) or at least 3 (E-F) independent experiments. Data are presented as mean ± SD (C-E,H). Statistical significance was calculated by 1-way ANOVA with Holm-Sidak multiple comparisons test (C,E,H) or unpaired 2-tailed Student *t* test (D).

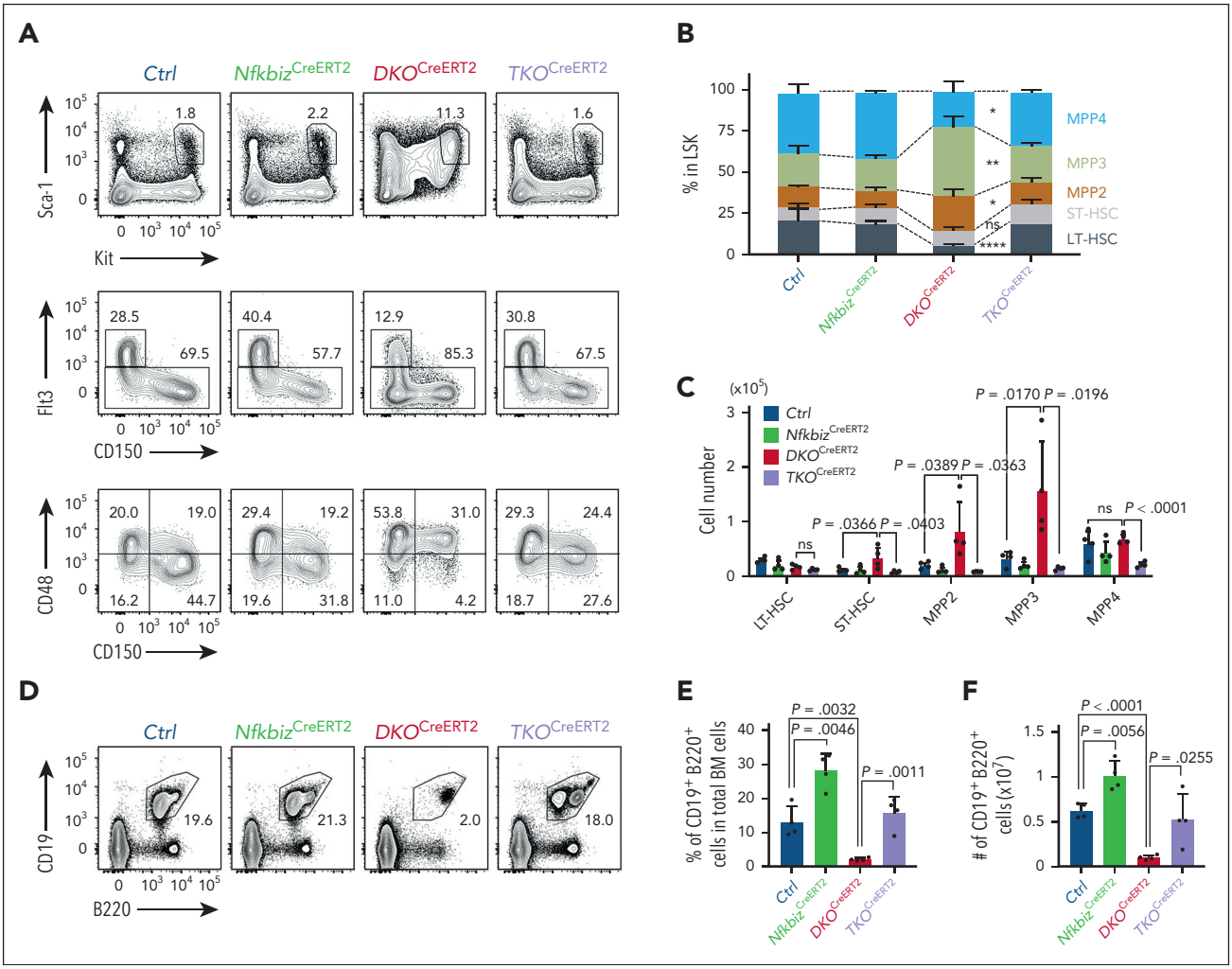

Figure 4. The Reg1/Reg3-*Nfkbiz* axis controls lymphoid-myeloid fate decision. (A-C) Representative flow cytometry plots (A), frequencies (B) and cell numbers (C) of HSPC subpopulations in mice of the indicated genotypes at day 14 after tamoxifen treatment. *Ctrl*, CreERT2^{+}*Reg1*$^{fl/+}$*Reg3*$^{+/+}$*Nfkbiz*$^{fl/+}$; *Nfkbiz*^{CreERT2}, CreERT2^{+}*Reg1*$^{fl/+}$*Reg3*$^{+/+}$*Nfkbiz*$^{fl/fl}$; *DKO*^{CreERT2}, CreERT2^{+}*Reg1*$^{fl/fl}$*Reg3*$^{-/-}$*Nfkbiz*$^{+/+}$; *TKO*^{CreERT2}, CreERT2^{+}*Reg1*$^{fl/fl}$*Reg3*$^{-/-}$*Nfkbiz*$^{fl/fl}$ (n = 4 each). Asterisks represents *P* value (*$P < .05$; **$P < .01$; ****$P < .0001$). (D-F) Representative flow cytometry plots (D), and frequency (E) and cell number (F) of B cells in the indicated mice (*n* = 4 each). (G-I) Representative flow cytometry plots (G) and frequencies (H) and cell numbers (I) of myeloid cells in the indicated mice (n = 4 each). (J-L) In vitro B-cell differentiation using Lin^{-}Kit^{+}IL-7Rα^{+} FL cells derived from the indicated genotypes. Progenitor cells were differentiated under B-cell–promoting condition in the presence of 4-OHT. *Ctrl*, CreERT2^{+}*Reg1*$^{fl/+}$*Reg3*$^{+/+}$*Nfkbiz*$^{fl/+}$; *Nfkbiz*^{CreERT2}, CreERT2^{+}*Reg1*$^{fl/+}$*Reg3*$^{+/+}$*Nfkbiz*$^{fl/fl}$; *DKO*^{CreERT2}, CreERT2^{+}*Reg1*$^{fl/fl}$*Reg3*$^{-/-}$*Nfkbiz*$^{+/+}$; *TKO*^{CreERT2}, CreERT2^{+}*Reg1*$^{fl/fl}$*Reg3*$^{-/-}$*Nfkbiz*$^{fl/fl}$. Representative flow cytometry plots (J), frequency (K), and absolute number (L) of CD19^{+}B220^{+} cells are shown. n = 6. Data are a composite of 2 independent experiments (A-I) or a representative of 2 independent experiments (J-L). Data are presented as mean ± SD (C,E-F,H-I,K-L). Statistical significance was calculated by 1-way ANOVA with Holm-Sidak multiple comparisons test. 4-OHT, 4-hydroxytamoxifen.

defined as long-term HSC (LT-HSC) (Flt3^{-}CD150^{+}CD48^{-}LSK), short-term HSC (ST-HSC) (Flt3^{-}CD150^{-}CD48^{-}LSK), MPP2 (Flt3^{-}CD150^{+}CD48^{+}LSK), MPP3 (Flt3^{-}CD150^{-}CD48^{+}LSK), MPP4 (Flt3^{+}CD150^{-}CD48^{+}LSK), and CLPs (Flt3^{+}IL-7Rα^{+}Lin^{-}Sca1^{dull}Kit^{dull}) (supplemental Figure 3E). *DKO*^{CreERT2} mice displayed a significant reduction in CLPs, whereas ST-HSC, MPP2, and MPP3 showed increased numbers compared with that of control mice (supplemental Figure 3F-G).

Taken together, our findings suggest that Reg1 and Reg3 are important for balancing lymphoid-myeloid differentiation in HSPCs.

Reg1 and Reg3 are required for the priming of lymphoid-biased HSPCs

Recent scRNA-seq approaches suggest that transcriptional lineage priming is initiated in HSPCs and is correlated with their functional lineage biases.[1,15,26,28] To investigate whether Reg1 and Reg3 contribute to shaping lineage biases in HSPCs, we performed scRNA-seq analysis of WT and *DKO* LSK cells containing HSCs and MPPs from competitively FL-transferred mice (Figure 2A). WT and *DKO* LSK populations were single cell–sorted into 384 well plates, and 2241 and 2242 cells were analyzed from each background, respectively (Figure 2B; supplemental Figure 4A). We used the MetaCell approach by which homologous populations were grouped based on similar transcriptional profiles to distinguish between closely related cell types (supplemental Figure 4B).[26] When WT and *DKO* cells were projected onto the hematopoietic core map,[26] *DKO* cells were enriched in the direction of myeloid and megakaryocytic-erythroid progenitors compared with control, whereas lymphoid lineages were underrepresented in *DKO* cells (Figure 2C). Consistently, meta cells representing myeloid- and

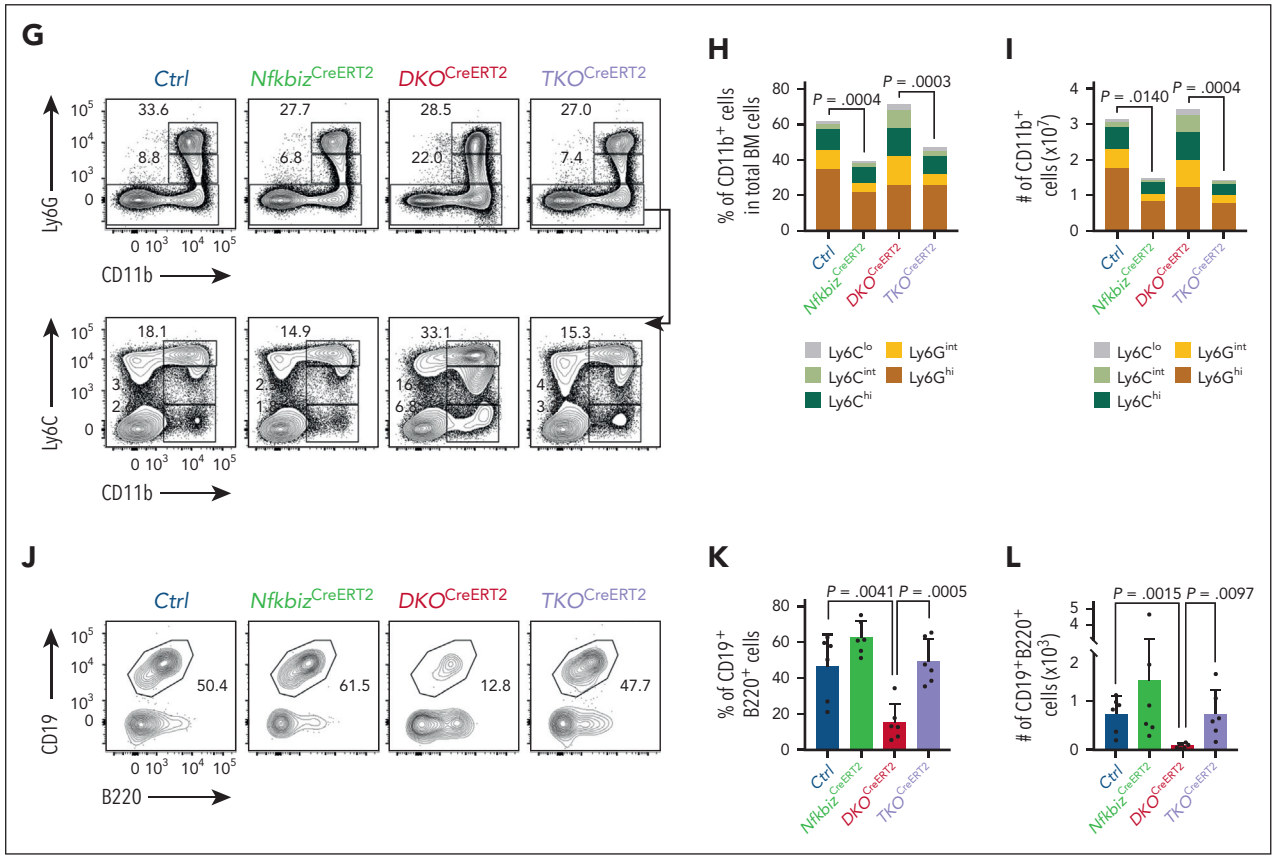

Figure 4 (continued)

megakaryocytic/erythroid-biased populations increased in *DKO* samples compared with that of WT, whereas those representing lymphoid populations decreased in *DKO* samples (Figure 2C-D; supplemental Figure 4C; supplemental Table 1). The expression levels of phenotypic markers for myeloid-biased HSCs, such as CD41, did not significantly increase in *DKO* cells (supplemental Figure 4D-F). Thus, our results support the notion that Reg1 and Reg3 are critical for the generation of B-lymphoid lineages from HSCs to maintain balanced hematopoiesis.

DKO HSCs shift toward myeloid-biased hematopoiesis upon serial transplantation

We further assessed the long-term maintenance of lineage-biased hematopoiesis in *DKO* HSCs by transplanting LT-HSCs isolated from CreERT2^{+} control or CreERT2^{+}*Reg1*$^{fl/fl}$*Reg3*$^{-/-}$ mice (*DKO*^{CreERT2}) along with supportive BM cells into lethally irradiated recipients (supplemental Figure 5A). *DKO*^{CreERT2} LT-HSCs gave rise to a higher percentage of granulocytes and monocytes and a lower percentage of B/T-lymphocytes than control after primary transplantation (supplemental Figure 5B). In secondary recipients, *DKO*^{CreERT2} LT-HSC–derived cells maintained skewed lineage outputs toward granulocytes and monocytes and away from B/T-lymphocytes, compared with that of control LT-HSC–derived cells (supplemental Figure 5C). Notably, the number of LT-HSCs was not altered 3 months after primary and secondary transplantation (supplemental Figure 5D-E). These finding indicate that myeloid-biased hematopoiesis persisted in the absence of *Reg1* and *Reg3* even after secondary transplantation.

Reg1 and Reg3 cooperatively regulate a set of mRNAs including *Nfkbiz* and *Ehd3*

We next explored how degradation of a common set of mRNAs in HSCs allows for Reg1 and Reg3 to prime and maintain B-lymphoid lineage–biased MPPs. We compared differentially expressed genes between WT and *DKO* HPSCs by reanalyzing the scRNA-seq data (supplemental Table 2). Remarkably, most of the upregulated genes in *DKO* cells were myeloid-lineage–associated genes, such as *Mpo*, *Ccl9*, *Ctsg*, *Ebi3*, and *Elane* (Figure 2F). In contrast, downregulated genes included *Dntt* and *Stmn1*, which are required for lymphoid development and suppression of megakaryocytic differentiation, respectively.[29,30] Consistently, *Mpo*, *Elane*, and *Ebi3* were highly expressed in myeloid and monocyte progenitors of *DKO* cells compared with WT counterparts (Figure 2G; supplemental Figure 6A). In addition to myeloid-associated genes, *Nfkbiz* and *Ehd3* were found to be upregulated in *DKO* cells (Figure 2F-G; supplemental Figure 6A). Interestingly, these genes were increased in *DKO* cells even in undetermined progenitors, which potentially contain HSCs, as well as lymphoid- and myeloid-biased progenitors (Figure 2G; supplemental Figure 6A). Quantitative PCR analysis using mixed chimera mice receiving WT and *DKO* FL cells confirmed a significant elevation of *Nfkbiz* and *Ehd3* in *DKO* CD150^{+}LSK and lymphoid primed multipotent progenitor (LMPP), compared with WT cells (supplemental Figure 6B). On the contrary, lineage-related TFs that can skew HSPC differentiation toward myeloid or megakaryocytic-erythroid lineages, including *Cebpa*, *Cebpb*, *Spi1*, and *Gata1*, were not altered between WT and *DKO* cells (supplemental Figure 6B).

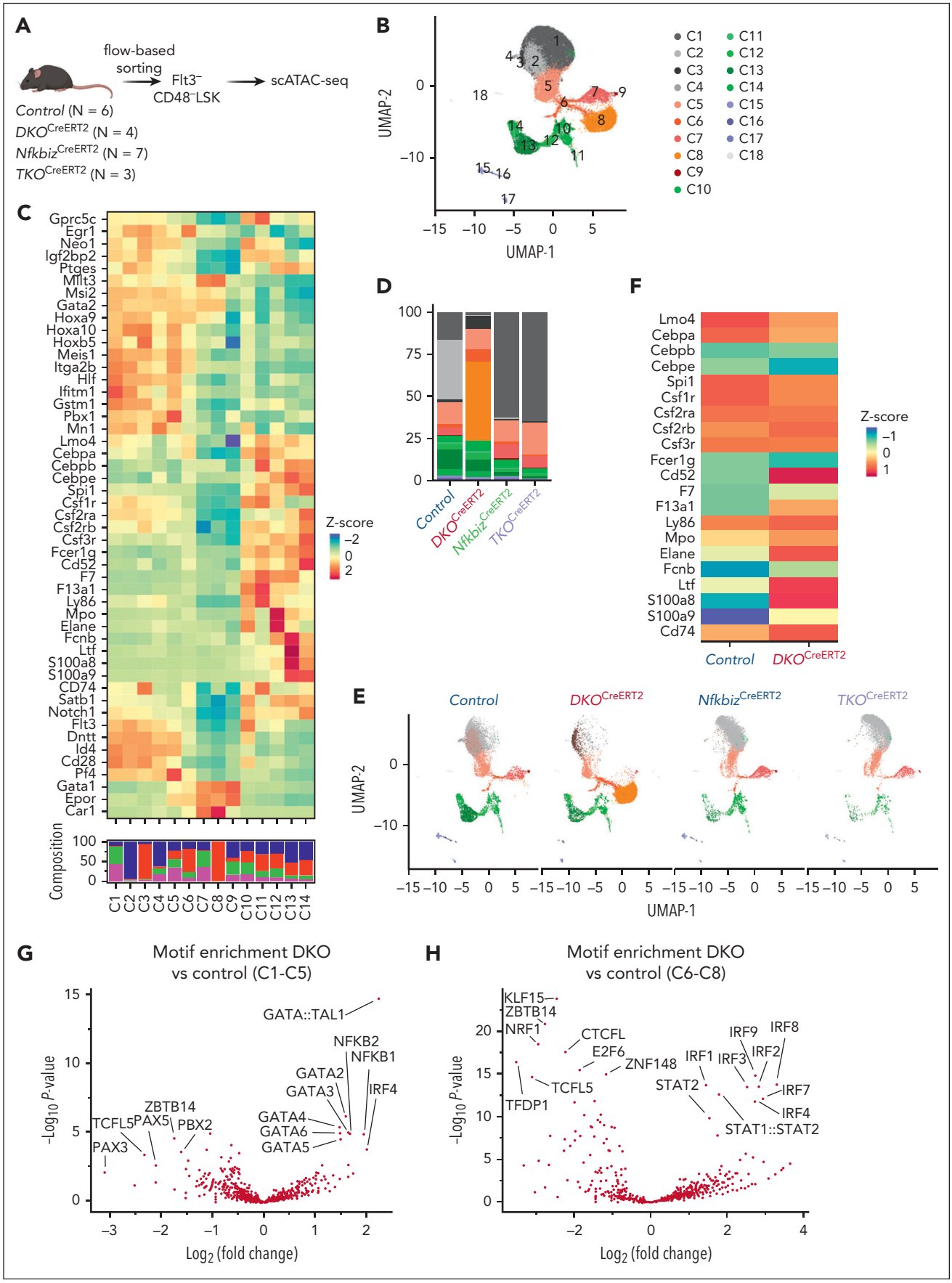

Figure 5.

Then, we examined whether the genes increased in *DKO* HSPCs were directly controlled by these RNases. Luciferase reporter experiments showed that both Reg1 and Reg3 inhibited the luciferase activity in cells expressing luciferase constructs harboring 3′ UTRs of *Nfkbiz* and *Ehd3* (Figure 2H). In contrast, nuclease-dead mutants of Reg1 (D141N) and Reg3 (D271N) failed to suppress the reporter activity, suggesting that Reg1 and Reg3 inhibited *Nfkbiz* and *Ehd3* in a manner dependent on their RNase enzymatic activities. The 3′ UTRs of *Irf8* and *Cebpd* were also responsive to the overexpression of Reg1 or Reg3, but no significant change in their gene expressions was observed in *DKO* progenitors (supplemental Figure 6B-C). However, *Reg1*/*Reg3*-doubly–deficient Lin$^-$ cells showed enhanced stability of *Nfkbiz* transcript and had only a partial effect on *Ehd3*, whereas the stability of *Irf8* or *Cebpd* mRNAs were not influenced by the double-deficiency of *Reg1* and *Reg3* (Figure 2I; supplemental Figure 6D), confirming that both Reg1 and Reg3 are required to downregulate or suppress *Nfkbiz* and *Ehd3* mRNA levels.

Reg1 and Reg3 control lymphoid-myeloid lineage balance via *Nfkbiz* in HSPCs

To investigate whether *Nfkbiz* or *Ehd3* influences lymphoid and/or myeloid differentiation in HSPCs, we used a culture system of mouse primary MPPs maintained by overexpressing human Id3-ERT2 fusion protein (MPP$^{hId3\text{-}ERT2}$) in the presence of 4-hydroxytamoxifen (Figure 3A).[31] We retrovirally expressed *Nfkbiz*, *Ehd3*, and TFs implicated in myeloid differentiation as controls in MPP$^{hId3\text{-}ERT2}$ cells. As expected, expression of myeloid master regulators, C/EBPα and C/EBPβ, strongly blocked B-cell differentiation and induced myeloid differentiation (Figure 3B-C). Interestingly, Nfkbiz expression in MPP$^{hId3\text{-}ERT2}$ cells resulted in a profound defect in lymphoid differentiation and promoted myeloid-lineage differentiation to a degree similar to the effects of C/EBPα and C/EBPβ, whereas Ehd3 showed only a modest effect on myeloid-lymphoid differentiation in MPP$^{hId3\text{-}ERT2}$ cells (Figure 3B-C). We then established MPP$^{hId3\text{-}ERT2}$ cells from *Reg1*$^{fl/fl}$*Reg3*$^{-/-}$ BM cells in which cre recombinase could be expressed by doxycycline (DOX) treatment in vitro (tetO-*cre*-*Reg1*$^{fl/fl}$*Reg3*$^{-/-}$ MPP$^{hId3\text{-}ERT2}$) (supplemental Figure 7A-C). Consistent with the hematopoietic changes in the BM caused by double-deficiency of *Reg1* and *Reg3*, tetO-*cre*-*Reg1*$^{fl/fl}$*Reg3*$^{-/-}$ MPP$^{hId3\text{-}ERT2}$ cells failed to induce CD19$^+$ cells but reciprocally increased CD11b$^+$ myeloid cells under B-cell differentiating condition in the presence of DOX (Figure 3D). The Nfkbiz expression was strikingly elevated after *Reg1* depletion both at mRNA and protein levels (Figure 3E-F). RNA-immunoprecipitation (IP) experiments showed that nuclease-dead mutants of Reg1 or Reg3 coprecipitated mRNA for *Nfkbiz* but not a Reg1 nontarget gene *Nfkbia* (Figure 3G-H), indicating that both Reg1 and Reg3 directly interact with *Nfkbiz* mRNA.

We then asked whether the lineage bias in hematopoiesis in the absence of *Reg1* and *Reg3* depends on in vivo *Nfkbiz* expression. For this purpose, we crossed *DKO*^{CreERT2} mice, which showed elevated Nfkbiz expression in Lin$^-$ BM cells (supplemental Figure 7D), with *Nfkbiz*$^{fl/fl}$ (*TKO*^{CreERT2}) mice and analyzed them at day14 after tamoxifen injection. Intriguingly, *TKO*^{CreERT2} mice showed a dramatic improvement in the frequencies and numbers of HSPC subpopulations compared with that of *DKO*^{CreERT2} mice (Figure 4A-C). In parallel, the frequency and number of CD19$^+$B220$^+$ B cells, as well as CD11b$^+$ myeloid cells, were fully restored in *TKO*^{CreERT2} mice (Figure 4D-I). Moreover, B-cell differentiation potential was also restored in *TKO*^{CreERT2} cells in an in vitro B-cell differentiation assay (Figure 4J-L), indicating that the upregulation of Nfkbiz accounts for the alteration in HSC lineage determination under the *Reg1*/*Reg3* double deficiency. Taken together, these findings demonstrate that the posttranscriptional control of *Nfkbiz* expression by Reg1 and Reg3 licenses lymphopoiesis by suppressing myeloid differentiation in HSPCs.

The Reg1/Reg3-*Nfkbiz* axis shapes epigenetic lineage priming in HSC

Because Nfkbiz acts as a transcriptional modulator inducing chromatin remodeling,[32,33] we hypothesized that the increased *Nfkbiz* expression modified epigenetic landscape in HSCs. To address this possibility, we examined the single-cell chromatin accessibility landscape using single cell-assay for transposase-accessible chromatin sequencing (scATAC-seq) of Flt3$^-$CD48$^-$ LSK population, which contains HSCs and the intermediate cells between HSCs and CD48$^+$ lineage-biased MPPs (Figure 5A).[34,35] We sequenced 13 859, 9936, 10 991, and 6902 cells for control, *Nfkbiz*^{CreERT2}, *DKO*^{CreERT2}, and *TKO*^{CreERT2}, respectively. Uniform Manifold approximation and projection (UMAP) plot for total cells showed that clustering based on the differential chromatin accessibilities generated 18 clusters (C1-C18) (Figure 5B). To dissect the chromatin accessibility profiles across the clusters, we examined the selected markers for HSCs and mature cell lineages.[26,36] The chromatin of stemness-related genes (*Hoxa9*, *Hoxa10*, *Gata2*, *Mllt3*, *Hlf*, *Meis1*, and *Msi2*) was more accessible in clusters C1 to C8 than in the rest of the clusters (Figure 5C; supplemental Figure 8A-C). In contrast, clusters C10 to C14 displayed distinct patterns of accessibilities in a set of myeloid-related genes (*Spi1*, *Csf1r*, *Csf2rb*, *Csf3r*, *F13a1*, and *Fcer1g*) and lymphoid-related genes (*Flt3* and *Satb1*) (Figure 5C; supplemental Figure 8A-C), suggesting that cells in these clusters harbor myeloid/lymphoid epigenetic features reminiscent of MPP5 and MPP6 that are phenotypically defined as CD34$^-$ and CD34$^+$ Flt3$^-$CD150$^-$CD48$^-$ LSK, respectively.[35] Among clusters C1 to C8, clusters C1 to C5 were consolidated in the UMAP plot and showed common features in the increased accessibility of lymphoid- and myeloid-related genes compared with that of clusters C6 to C8 (Figure 5B-C). In contrast, erythroid-related

Figure 5. The Reg1/Reg3-*Nfkbiz* axis regulates lineage priming of HSCs/early MPPs via chromatin remodeling. (A) Schematic representation of scATAC-seq using Flt3$^-$CD48$^-$ LSK. In each genotype, samples are pooled from multiple mice to create a single sample for sequencing, as indicated by the number of mice represented. (B) UMAP visualization of all cells obtained from scATAC-seq data. Colors represent the cluster identity. (C) Heatmap showing chromatin accessibility for stemness-related and lineage-associated genes. (D) Cluster distribution of single cells across the indicated genotypes. Colors represent the cluster identity as in (B). (E) A 2-dimensional projection of 13859, 10991, 9936, and 6902 single cells from control, *DKO*^{CreERT2}, *Nfkbiz*^{CreERT2}, and *TKO*^{CreERT2}, respectively, onto the UMAP plot (B). (F) Heatmap showing differential chromatin accessibilities of the selected myeloid-related gene loci between control and *DKO*^{CreERT2} cells in C1 to C5. (G-H) Volcano plot showing the comparison of TF motif enrichment between control vs *DKO*^{CreERT2} in C1 to C5 (G) and C6 to C8 (H).

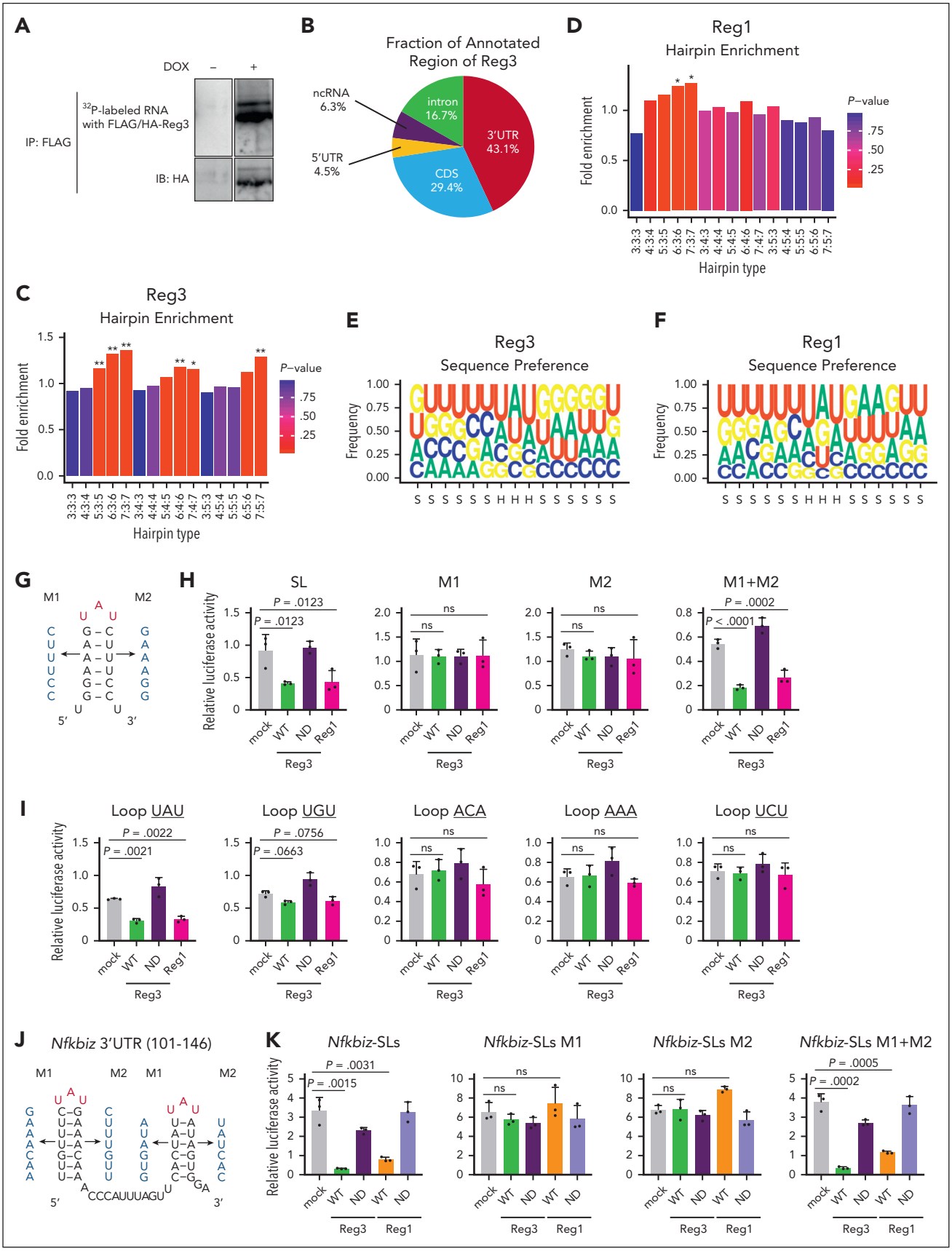

Figure 6. Reg1 and Reg3 recognize the tandem UAU-SL structures present in the *Nfkbiz* 3′ UTR. (A) Phosphoimage of SDS-PAGE of radiolabelled Reg3-RNA complexes obtained by immunoprecipitation with anti-FLAG antibody. (B) Pie chart deciphering the distribution of Reg3-binding sites obtained by the intersection of 2 biological

genes (*Gata1*, *Epor*, and *Car1*) were accessible in clusters C6 to C8 (Figure 5C).

The chromatin accessibility landscape was dramatically altered in $DKO^{CreERT2}$ cells characterized by their dominance in C3 and C8 together with the underrepresentation of C1, C2, C4, C5, and C7 (Figure 5D-E). In contrast, $DKO^{CreERT2}$ cells were evenly observed in clusters C10 to C14. Interestingly, $DKO^{CreERT2}$ cells showed more accessibility for myeloid-related genes such as *Cd74* and *Csf2rb* in clusters C1 to C8 than control (Figure 5C,F). Notably, the changes in chromatin accessibility in *DKO* cells were drastically restored by further deletion of *Nfkbiz*, implying that Reg1 and Reg3 regulate epigenetic homeostasis in HSCs by suppressing the expression of *Nfkbiz* (Figure 5D-F).

Consistent with the role of Nfkbiz in controlling gene expression via interaction with TFs such as NF-κB, NF-κB–binding motifs were enriched in regions more accessible in $DKO^{CreERT2}$ cells than in control cells in clusters C1 to C5 (Figure 5G). Furthermore, GATA and IRF family–binding motifs were also more frequently observed in regions highly accessible in $DKO^{CreERT2}$ cells in clusters C1 to C5 and C6 to C8, respectively (Figure 5G-H). These findings suggest that the activation of Nfkbiz in $DKO^{CreERT2}$ cells can facilitate the recruitment of TFs involved in lineage priming via chromatin remodeling.

Reg3 and Reg1 recognize and destabilize mRNAs with common signatures

Next, we analyzed the mechanisms of how Reg1 and Reg3 recognize target mRNAs. Because Reg1-interacting stem-loop motifs were identified by high-throughput sequencing of cross-linking and IP (HITS-CLIP) analyses,[23] we analyzed the transcriptome-wide binding mode of Reg3 with the same technique. To this end, HEK293T cells stably expressing DOX-inducible FLAG-tagged Reg3 were generated and UV cross-linked. IP of FLAG-Reg3 yielded Reg3-RNA complexes after induction of Reg3 by DOX treatment (Figure 6A). Recovered RNA fragments from 2 independent HITS-CLIP experiments were deep sequenced, and genome-aligned reads were clustered, allowing for the identification of 6639 and 7678 putative Reg3-binding sites in 2 biological duplicate libraries, respectively (supplemental Table 3). We found that the uniquely mapped reads of Reg3-binding sites were enriched in 3′ UTRs (Figure 6B). When the secondary structures of these sequences were analyzed by RNAfold,[37] SL structures with 3 to 7 nucleotide stems and trinucleotide loops were significantly enriched (Figure 6C). In addition, motif analyses of the SL sequences revealed that the uridine-adenine-uridine (UAU) triplet was overrepresented in the hairpin sequences of Reg3-binding motifs (Figure 6E). This is reminiscent of the Reg1-binding motifs revealed by the HITS-CLIP analysis (Figure 6D,F).[23] Interestingly, Reg3- and Reg1-binding sequences overlapped significantly (supplemental Table 4), indicating that Reg3 and Reg1 target an overlapping set of mRNAs by recognizing a common binding motif.

Consistently, a luciferase reporter RNA harboring the SL-containing sequence with an UAU-loop sequence in the 3′ UTR was suppressed by the overexpression of either RNase-competent Reg3 or Reg1 (Figure 6G-H). Disruption of the SL structure by mutating either side of the stem sequence abrogated the Reg3-mediated suppression of the luciferase activity (Figure 6G-H). Restoration of the SL structure by mutating both sides of the stem sequences restored Reg3 responsiveness (Figure 6H). SLs harboring UAU and, to a lesser extent, UGU, but not ACA, AAA or UCU, were suppressed by Reg3, suggesting that the pyrimidine-purine-pyrimidine loop sequences are required for Reg3 suppression, similar to Reg1 (Figure 6I). These results demonstrate that Reg3 and Reg1 recognize overlapping sets of mRNAs by recognizing common SL sequences present in the mRNA 3′ UTR.

Next, we investigated SL structure(s) in the *Nfkbiz* 3′ UTR responsible for the Reg1/Reg3-mediated decay. Luciferase reporter assays revealed that the *Nfkbiz* instability element was located within the 1 to 200 region of its 3′ UTR and contains 4 SL structures (SL1-SL4) (supplemental Figure 9A-B). Among these, SL3 and SL4, but not SL1 and SL2, were responsible for the suppression by both Reg1 and Reg3 (supplemental Figure 9C). These SLs harbor UAU-loop sequences (supplemental Figure 9B), a consensus motif for Reg1 and Reg3 recognition (Figure 6E-F). Consistently, a reporter containing either SL3 or SL4 was suppressed by the overexpression of Reg1 or Reg3 (supplemental Figure 9D). The Reg1/Reg3 responsiveness of SL3 and SL4 was abrogated by mutation of SL structures and was rescued by restoration of SL structures by introducing mutations in both sides of the stem sequences (Figure 6J-K), indicating that Reg1 and Reg3 commonly recognize SL structures in SL3 and SL4 for degrading *Nfkbiz*.

Enhancement of *Nfkbiz* expression via its 3′ UTR leads to myeloid priming in HSCs

The aforementioned results prompted us to hypothesize that enhancement of *Nfkbiz* expression by inhibiting Reg1/Reg3-mediated decay could control HSC lineage bias. We achieved an increase in Reg1 expression by targeting its self-regulation through the use of ASOs against SL structures located in the

Figure 6 (continued) HITS-CLIP replicates. (C-D) SL enrichments in Reg3- and Reg1-bound CLIP tags of the 3′ UTR compared with 1000 individual sequence permutations. X-axis indicates hairpin types in which the numbers represent the lengths of stem and loop. *$P < .01$; **$P < .001$. (E-F) Sequence logo representations of the recognition motives for Reg3 and Reg1. Stem and hairpin regions are indicated as S and H, respectively, below the x-axis. (G) Schematic representation of the artificial SL structure and its mutant forms (M1 and M2) in which the SL structure is disrupted. (H) Luciferase activity was assessed by using pGL3-βGlo plasmids containing the 3′ UTR with SL, M1, M2, and M1+ M2 as shown in (G). HeLa cells were transfected with pGL3 plasmids together with expression plasmids for WT Reg1, WT, or ND mutant of Reg3 (n = 3 each). (I) Luciferase activity was assessed by using pGL3-βGlo plasmids containing the 3′ UTR with a set of loop sequences. The loop sequences tested are shown in the top of figures. Transfection was performed as in (H) (n = 3 each). (J) Schematic representation of mouse *Nfkbiz* SL structures targeted by Reg1 and Reg3. M1 and M2 represent mutant sequences that no longer form SL structures. (K) Luciferase activity was assessed by using pGL3-βGlo plasmids containing either WT or mutated SL sequences (M1, M2, or M1+ M2) as shown in (J). HeLa cells were transfected with pGL3 plasmids together with expression plasmids for WT or ND mutant of Reg1 and Reg3 (n = 3 each). Data are representative of 2 to 3 independent experiments (H-I,K). Data are presented as mean ± SD (H-I,K). Statistical significance was calculated by 1-way ANOVA with Holm-Sidak multiple comparisons test (H-I,K).

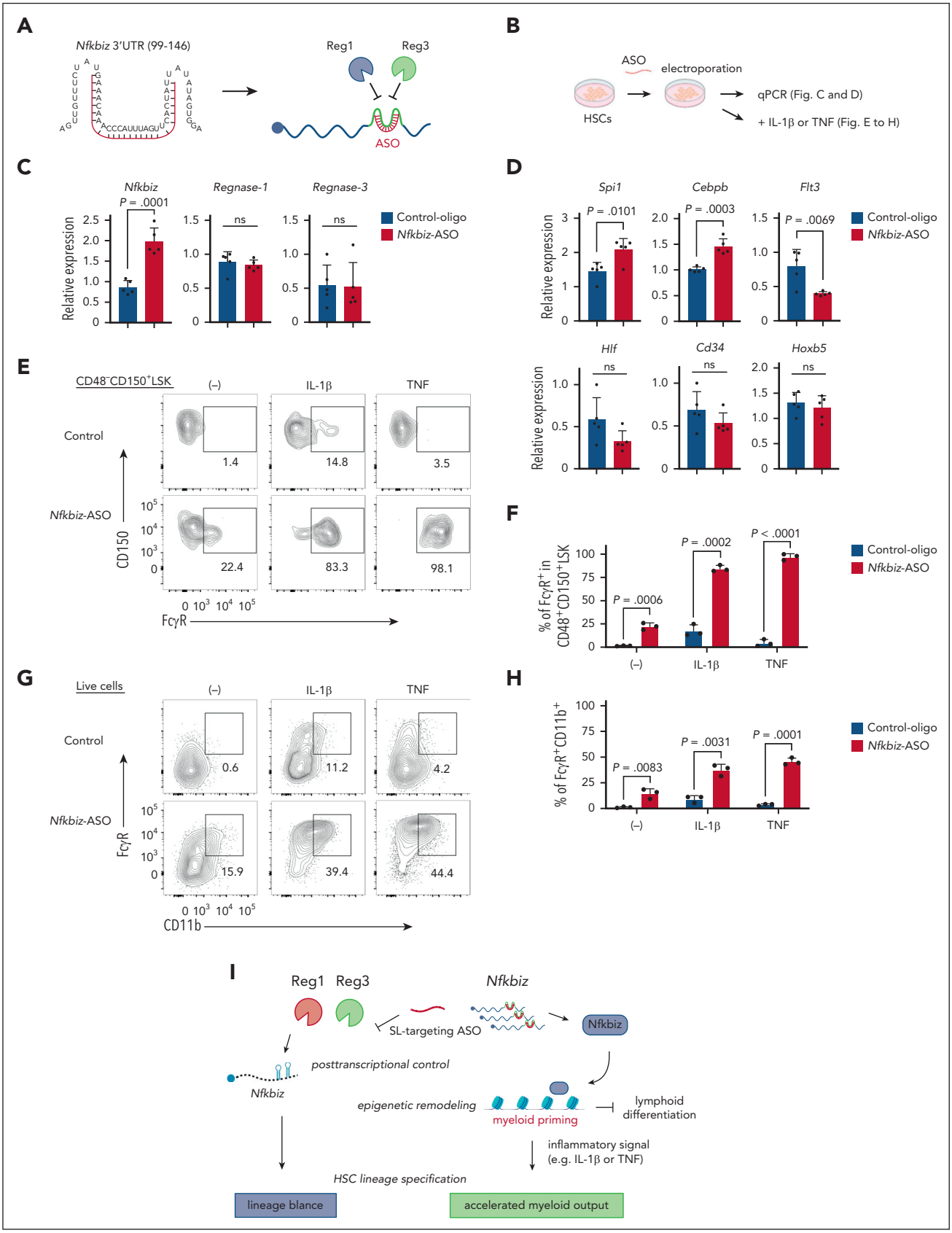

Figure 7. Manipulation of *Nfkbiz* expression by ASO alters HSC lineage priming toward myeloid lineage. (A) Schematic representation of ASO (shown in red) for Reg1/Reg3-targeting SL structures in the mouse *Nfkbiz* 3′ UTR. (B) Experimental design for ASO-transduced HSCs. HSCs were electroporated with control oligo or *Nfkbiz*-targeting ASO. Cells were used for subsequent analyses in (C-H). (C-D) qRT-PCR analysis of *Nfkbiz*, *Reg1*, *Reg3* and HSC/lineage-related genes in cultured HSCs at day 5 after electroporation (n = 5 each). (E-F) Representative flow cytometry plots and frequency of FcγR expression in CD48⁻CD150⁺ LSK from cultured HSCs stimulated with IL-1β or TNF

Reg1 3′ UTR.[38] To inhibit Reg1/Reg3-mediated *Nfkbiz* mRNA decay, we designed morpholino ASOs to target and disrupt the SL structures of SL1, SL2, andSL3-4 (supplemental Figure 9B). Because SL3 and SL4 aligned tandemly with a short interval, we designed an ASO targeting both SL3 and SL4 (Figure 7A). When we introduced ASOs together with the reporter harboring the full-length *Nfkbiz* 3′ UTR, the SL3-4–targeting ASO highly increased luciferase activity compared with control-oligo or ASOs against SL1 or SL2 (supplemental Figure 10A). The results suggest that the SL3-4–targeting ASO (hereafter *Nfkbiz*-ASO) is potent to stabilize *Nfkbiz* mRNA by altering the SL structure. Similarly, in BM-derived macrophages, the *Nfkbiz*-ASO stabilized *Nfkbiz* mRNA and enhanced *Nfkbiz* expression both at mRNA and protein levels (supplemental Figure 10B-D). Consistent with the proinflammatory function of Nfkbiz in macrophages, the *Nfkbiz*-ASO augmented IL-6 production after lipopolysaccharide (LPS) treatment (supplemental Figure 10E). In contrast, *Nfkbiz*-ASO failed to increase *Nfkbiz* expression in *Reg1/Reg3 DKO* macrophages (supplemental Figure 10F), suggesting that the ASO enhanced *Nfkbiz* expression by inhibiting Reg1/Reg3-mediated mRNA decay.

Next, we investigated whether the *Nfkbiz*-ASO is also potent to increase the *Nfkbiz* expression in HSC by using a serum-free HSC culture system that enables efficient enrichment of $CD150^{+}CD48^{-}CD201^{+}$ LSK population (Figure 7B; supplemental Figure 10G-H).[39] We found that a Fluorescein isothiocyanate (FITC)-conjugated ASO was efficiently introduced into cultured HSCs (cHSCs) by electroporation and persisted at least for 5 days (supplemental Figure 10I-J). As expected, the introduction of the *Nfkbiz*-ASO enhanced the expression of *Nfkbiz* in cHSCs compared with SL1- or SL2-targeting ASOs (Figure 7C; supplemental Figure 10K). In contrast, the *Nfkbiz*-ASO did not influence the expression of Reg1 or Reg3, suggesting that the ASO specifically acts on *Nfkbiz* transcripts. Interestingly, *Nfkbiz*-ASO treatment for 5 days mildly but significantly enhanced the expression of myeloid-related genes *Spi1* and *Cebpb*, whereas the treatment reduced *Flt3* expression in cHSCs (Figure 7D). Consistently, cell surface expression of FcγR, a myeloid marker, was slightly augmented in $CD150^{+}CD48^{-}$ LSK population by treatment with *Nfkbiz*-ASO (Figure 7E-F). In contrast, the *Nfkbiz*-ASO did not alter the expression of HSC-related genes including *Hlf*, *Cd34*, and *Hoxb5* (Figure 7D) or the frequency of LSK population (supplemental Figure 10L-M). Although *Nfkbiz*-ASO treatment alone slightly induced myeloid differentiation, simultaneous treatment with TNF or IL-1β drastically promoted myeloid differentiation of cultured HSCs (Figure 7G-H). Interestingly, TNF or IL-1β synergized with *Nfkbiz*-ASO and dramatically enhanced FcγR expression in $CD150^{+}CD48^{-}$ LSK population of cHSCs (Figure 7E-F). Taken together, the *Nfkbiz*-ASO is potent to induce myeloid-lineage priming in HSCs by enhancing the expression of Nfkbiz.

Discussion

In this study, we discovered that the Reg1/Reg3-*Nfkbiz* axis acts as the novel regulatory mechanism governing lineage bias in HSPCs, identifying it as a promising target for manipulating hematopoiesis (Figure 7I). It was demonstrated that epigenetic regulation is critical for the lineage specification of HSPCs, and it is difficult to separate these features of stem cells by known epigenetic factors.[40-43] In this regard, we believe that Reg1 and Reg3 are novel cellular factors to be identified that determine myeloid-lymphoid cell fate decision by controlling HSPCs.

Despite the multiple functions of *Nfkbiz* in various mature immune cells,[32,44-46] its role in HSCs has not yet been discussed. The IκB-ζ protein, encoded by the *Nfkbiz* gene, interacts with NF-κBp50 to reinforce NF-κB activation[32] and also participates in chromatin remodeling under inflammatory conditions.[44,46] NF-κB has been shown to be involved in emergency myelopoiesis by TNF,[16] and the cooperation between NF-κBp50 and C/EBPα in the granulocytic progenitors for promoting myelopoiesis has been demonstrated.[47] Therefore, *Nfkbiz* expressed by the suppression of Reg1/Reg3 may initiate the myeloid program in cooperation with the NF-κB and/or by recruiting the chromatin remodelers to induce epigenetic changes.

The Reg1/Reg3-*Nfkbiz* regulatory axis is a novel therapeutic target to manipulate myeloid- and lymphoid-biased outputs in hematopoiesis. We found that an ASO disrupting SL structures in the *Nfkbiz* 3′ UTR is potent to increase *Nfkbiz* expression and induce myeloid-biased lineage priming in HSCs. Given that this ASO specifically targets *Nfkbiz* expression, this strategy might be beneficial compared with the treatment with cytokines/TLR ligands, which can induce broad responses. Indeed, the SL structures targeted by Reg1 and Reg3 are conserved in human *NFKBIZ*. Nevertheless, further studies are required to optimize the sequences and nucleic acids modification as well as drug delivery to improve the efficacy of the therapeutic potential.

In summary, we demonstrate here that Reg1 and Reg3 act as molecular switch to control lineage biases in HSPCs by shaping transcriptional lineage priming. These 2 RNases control multipotent cell lineage choice by targeting *Nfkbiz* for degradation. *Nfkbiz* acts as a key regulator to promote myeloid-lineage commitment. Our findings provide insights into how HSC-lineage priming is regulated.

Acknowledgments

The authors thank H. Miyachi, S. Kitano, R. Takeda, and S. Nagai for animal technical service; T. Maruyama for providing *Nfkbiz* flox mice; Y. Agata for plasmid construction of retroviral expression of human *Id3*, S. Yamazaki for Soluplus, T. Nagasawa, N. Chevrier, and all members of the Takeuchi laboratory for insights and suggestions. Flow cytometric analysis and cell sorting using LSRFortessa (BD Biosciences) and AriaIII (BD Biosciences) were performed at the Medical Research Support Center, Graduate School of Medicine, Kyoto University, which was supported by Platform Project for Supporting Drug Discovery and Life Science Research (Basis for Supporting Innovative Drug Discovery and Life Science Research) from Japan Agency for Medical Research and Development (AMED) (grant number JP20am0101092). Figures were created using BioRender.com.

This study was supported by Japan Society for the Promotion of Science KAKENHI (18H05278, 23H00402) (O.T.) and (18K15185) (T.U.) and

Figure 7 (continued) for 24 hours (n = 3 each). (G-H) Representative flow cytometry plots and frequency of $FcγR^{+}CD11b^{+}$ cells from cultured HSCs stimulated with IL-1β or TNF for 24 hours (n = 3 each). (I) Model of the Reg1/Reg3-*Nfkbiz* axis in the control of HSC lineage priming. Data are representative of 3 independent experiments (C-H). Data are presented as mean ± SD (C-D,F,H) Statistical significance was calculated by unpaired 2-tailed Student *t* test (C-D,F,H).

Core-to-Core Program (O.T.) and grant-in-aid for Scientific Research on Innovative Areas 'Genome Science' (221S0002, 16H06279) (T.M.). This study was also supported by AMED (grant numbers JP20gm4010002, JP21ae0121030, 23ama221327h0001) (O.T.) and the Cooperative Research Program (Joint Usage/Research Center program) of Institute for Frontier Life and Medical Sciences, Kyoto University (O.T.) and a grant-in-aid for Transformative Research Areas (A) "Material Symbiosis" (grant 20H05874) (T.U.) and ISHIZUE 2017 of Kyoto University Research Development Program (T.U.), an Office of Directors' Research Grant provided by the Institute for Frontier Life and Medical Sciences, Kyoto University (A.V.), and the Fujiwara Memorial Foundation (T.U.).

Authorship

Contribution: T.U. and O.T. were in charge of experimental designs, analyses, interpretation of data, and drafting of the manuscript; S.Y., D.O., K. Toratani, and M.M. participated in the acquisition, analysis, and interpretation of data; A.J., A.G., and I.A. handled single cell RNA-sequencing (scRNA-seq) samples and performed analyses on scRNA-seq data; A.V. and K. Takeuchi. performed analysis of scRNA-seq and scATAC-seq (single-cell sequencing assay for transposase-accessible chromatin) data; Y.M. and M.L. performed HITS-CLIP (high-throughput sequencing of RNA isolated by crosslinking immunoprecipitation) of Reg3; H. Kiryu analyzed HITS-CLIP of Reg1 and Reg3; H.W. and G.K. contributed to genetic engineering to generate multiple mouse lines; T.T. performed histological examination; T.I. and R.Y. contributed to in vitro culture of multipotent progenitors and hematopoietic stem cells, respectively; D.M.S. carried out structural modeling; T.M., M.M., R.Y., H.-R.R., and H. Kawamoto provided critical discussions and suggestions; and O.T. supervised the overall study.

Conflict-of-interest disclosure: The authors declare no competing financial interests.

The current affiliation for D.O. is Laboratory of Molecular Immunobiology, Division of Biological Science, Graduate School of Science and Technology, Nara Institute of Science and Technology, Ikoma, Nara, Japan.

ORCID profiles: T.U., 0000-0003-3517-2198; D.O., 0000-0002-2535-7837; A.V., 0000-0003-2180-5732; A.G., 0000-0002-5880-2845; K.T., 0000-0002-1646-9167; T.M., 0000-0002-9562-008X; H.K., 0000-0003-3554-5353; M.L., 0000-0002-1075-8734; M.M., 0000-0002-9543-624X; O.T., 0000-0002-1260-6232.

Correspondence: Osamu Takeuchi, Department of Medical Chemistry, Graduate School of Medicine, Kyoto University, Yoshida-Konoe-cho, Sakyo-ku, Kyoto 606-8501, Japan; email: otake@mfour.med.kyoto-u.ac.jp.

Footnotes

Submitted 20 April 2023; accepted 17 October 2023; prepublished online on *Blood* First Edition 3 November 2023. https://doi.org/10.1182/blood.2023020903.

*T.U. and S.Y. contributed equally to this study.

Data for single cell RNA sequencing and single-cell sequencing assay for transposase-accessible chromatin have been deposited in the National Center for Biotechnology Information's Gene Expression Omnibus under accession codes GSE228923 and GSE229065, respectively.

Mouse strains generated in this work are available for noncommercial research purposes following a reasonable request. Source data are provided with this article. Data are available on request from the corresponding author, Osamu Takeuchi (otake@mfour.med.kyoto-u.ac.jp).

The online version of this article contains a data supplement.

There is a *Blood* Commentary on this article in this issue.

The publication costs of this article were defrayed in part by page charge payment. Therefore, and solely to indicate this fact, this article is hereby marked "advertisement" in accordance with 18 USC section 1734.

REFERENCES

1. Haas S, Trumpp A, Milsom MD. Causes and consequences of hematopoietic stem cell heterogeneity. *Cell Stem Cell*. 2018;22(5):627-638.
2. Höfer T, Rodewald HR. Differentiation-based model of hematopoietic stem cell functions and lineage pathways. *Blood*. 2018;132(11):1106-1113.
3. Olson OC, Kang YA, Passegué E. Normal hematopoiesis is a balancing act of self-renewal and regeneration. *Cold Spring Harb Perspect Med*. 2020;10(12):a035519.
4. Pina C, Fugazza C, Tipping AJ, et al. Inferring rules of lineage commitment in haematopoiesis. *Nat Cell Biol*. 2012;14(3):287-294.
5. Macaulay IC, Svensson V, Labalette C, et al. Single-cell RNA-sequencing reveals a continuous spectrum of differentiation in hematopoietic cells. *Cell Rep*. 2016;14(4):966-977.
6. Nestorowa S, Hamey FK, Pijuan Sala B, et al. A single-cell resolution map of mouse hematopoietic stem and progenitor cell differentiation. *Blood*. 2016;128(8):e20-31.
7. Velten L, Haas SF, Raffel S, et al. Human haematopoietic stem cell lineage commitment is a continuous process. *Nat Cell Biol*. 2017;19(4):271-281.
8. Olsson A, Venkatasubramanian M, Chaudhri VK, et al. Single-cell analysis of mixed-lineage states leading to a binary cell fate choice. *Nature*. 2016;537(7622):698-702.
9. Paul F, Arkin Y, Giladi A, et al. Transcriptional heterogeneity and lineage commitment in myeloid progenitors. *Cell*. 2016;164(1-2):325.
10. Hirai H, Zhang P, Dayaram T, et al. C/EBPbeta is required for 'emergency' granulopoiesis. *Nat Immunol*. 2006;7(7):732-739.
11. King KY, Goodell MA. Inflammatory modulation of HSCs: viewing the HSC as a foundation for the immune response. *Nat Rev Immunol*. 2011;11(10):685-692.
12. Mossadegh-Keller N, Sarrazin S, Kandalla PK, et al. M-CSF instructs myeloid lineage fate in single haematopoietic stem cells. *Nature*. 2013;497(7448):239-243.
13. Manz MG, Boettcher S. Emergency granulopoiesis. *Nat Rev Immunol*. 2014;14(5):302-314.
14. Pietras EM, Mirantes-Barbeito C, Fong S, et al. Chronic interleukin-1 exposure drives haematopoietic stem cells towards precocious myeloid differentiation at the expense of self-renewal. *Nat Cell Biol*. 2016;18(6):607-618.
15. Chavakis T, Mitroulis I, Hajishengallis G. Hematopoietic progenitor cells as integrative hubs for adaptation to and fine-tuning of inflammation. *Nat Immunol*. 2019;20(7):802-811.
16. Yamashita M, Passegue E. TNF-alpha coordinates hematopoietic stem cell survival and myeloid regeneration. *Cell Stem Cell*. 2019;25(3):357-372.e7.
17. Collins A, Mitchell CA, Passegué E. Inflammatory signaling regulates hematopoietic stem and progenitor cell development and homeostasis. *J Exp Med*. 2021;218(7):e20201545.
18. Beerman I, Bock C, Garrison BS, et al. Proliferation-dependent alterations of the DNA methylation landscape underlie hematopoietic stem cell aging. *Cell Stem Cell*. 2013;12(4):413-425.
19. Cullen SM, Mayle A, Rossi L, Goodell MA. Hematopoietic stem cell development: an epigenetic journey. *Curr Top Dev Biol*. 2014;107:39-75.
20. Sun D, Luo M, Jeong M, et al. Epigenomic profiling of young and aged HSCs reveals concerted changes during aging that reinforce self-renewal. *Cell Stem Cell*. 2014;14(5):673-688.
21. Uehata T, Takeuchi O. Post-transcriptional regulation of immunological responses by regnase-1-related RNases. *Int Immunol*. 2021;33(12):859-865.

22. Mino T, Iwai N, Endo M, et al. Translation-dependent unwinding of stem-loops by UPF1 licenses regnase-1 to degrade inflammatory mRNAs. *Nucleic Acids Res*. 2019;47(16):8838-8859.

23. Mino T, Murakawa Y, Fukao A, et al. Regnase-1 and roquin regulate a common element in inflammatory mRNAs by spatiotemporally distinct mechanisms. *Cell*. 2015;161(5):1058-1073.

24. Matsushita K, Takeuchi O, Standley DM, et al. Zc3h12a is an RNase essential for controlling immune responses by regulating mRNA decay. *Nature*. 2009;458(7242):1185-1190.

25. Uehata T, Iwasaki H, Vandenbon A, et al. Malt1-induced cleavage of regnase-1 in CD4(+) helper T cells regulates immune activation. *Cell*. 2013;153(5):1036-1049.

26. Giladi A, Paul F, Herzog Y, et al. Single-cell characterization of haematopoietic progenitors and their trajectories in homeostasis and perturbed haematopoiesis. *Nat Cell Biol*. 2018;20(7):836-846.

27. Baran Y, Bercovich A, Sebe-Pedros A, et al. MetaCell: analysis of single-cell RNA-seq data using K-nn graph partitions. *Genome Biol*. 2019;20(1):206.

28. Jacobsen SEW, Nerlov C. Haematopoiesis in the era of advanced single-cell technologies. *Nat Cell Biol*. 2019;21(1):2-8.

29. Iancu-Rubin C, Gajzer D, Tripodi J, et al. Down-regulation of stathmin expression is required for megakaryocyte maturation and platelet production. *Blood*. 2011;117(17):4580-4589.

30. Klein F, Roux J, Cvijetic G, et al. Dntt expression reveals developmental hierarchy and lineage specification of hematopoietic progenitors. *Nat Immunol*. 2022;23(4):505-517.

31. Ikawa T, Masuda K, Huijskens M, et al. Induced developmental arrest of early hematopoietic progenitors leads to the generation of leukocyte stem cells. *Stem Cell Reports*. 2015;5(5):716-727.

32. Yamamoto M, Yamazaki S, Uematsu S, et al. Regulation of Toll/IL-1-receptor-mediated gene expression by the inducible nuclear protein IkappaBzeta. *Nature*. 2004;430(6996):218-222.

33. Kayama H, Ramirez-Carrozzi VR, Yamamoto M, et al. Class-specific regulation of pro-inflammatory genes by MyD88 pathways and IkappaBzeta. *J Biol Chem*. 2008;283(18):12468-12477.

34. Pietras EM, Reynaud D, Kang YA, et al. Functionally distinct subsets of lineage-biased multipotent progenitors control blood production in normal and regenerative conditions. *Cell Stem Cell*. 2015;17(1):35-46.

35. Sommerkamp P, Romero-Mulero MC, Narr A, et al. Mouse multipotent progenitor 5 cells are located at the interphase between hematopoietic stem and progenitor cells. *Blood*. 2021;137(23):3218-3224.

36. Ranzoni AM, Tangherloni A, Berest I, et al. Integrative single-cell RNA-seq and ATAC-seq analysis of human developmental hematopoiesis. *Cell Stem Cell*. 2021;28(3):472-487.e7.

37. Lorenz R, Bernhart SH, Höner Zu Siederdissen C, et al. ViennaRNA package 2.0. *Algorithms Mol Biol*. 2011;6:26.

38. Tse KM, Vandenbon A, Cui X, et al. Enhancement of regnase-1 expression with stem loop-targeting antisense oligonucleotides alleviates inflammatory diseases. *Sci Transl Med*. 2022;14(644):eabo2137.

39. Wilkinson AC, Ishida R, Kikuchi M, et al. Long-term ex vivo haematopoietic-stem-cell expansion allows nonconditioned transplantation. *Nature*. 2019;571(7763):117-121.

40. Ko M, Bandukwala HS, An J, et al. Ten-eleven-translocation 2 (TET2) negatively regulates homeostasis and differentiation of hematopoietic stem cells in mice. *Proc Natl Acad Sci U S A*. 2011;108(35):14566-14571.

41. Challen GA, Sun D, Mayle A, et al. Dnmt3a and Dnmt3b have overlapping and distinct functions in hematopoietic stem cells. *Cell Stem Cell*. 2014;15(3):350-364.

42. Lara-Astiaso D, Weiner A, Lorenzo-Vivas E, et al. Immunogenetics. Chromatin state dynamics during blood formation. *Science*. 2014;345(6199):943-949.

43. Avgustinova A, Benitah SA. Epigenetic control of adult stem cell function. *Nat Rev Mol Cell Biol*. 2016;17(10):643-658.

44. Miyake T, Satoh T, Kato H, et al. IkappaBzeta is essential for natural killer cell activation in response to IL-12 and IL-18. *Proc Natl Acad Sci U S A*. 2010;107(41):17680-17685.

45. Okamoto K, Iwai Y, Oh-Hora M, et al. IkappaBzeta regulates T(H)17 development by cooperating with ROR nuclear receptors. *Nature*. 2010;464(7293):1381-1385.

46. Tartey S, Matsushita K, Vandenbon A, et al. Akirin2 is critical for inducing inflammatory genes by bridging IkappaB-zeta and the SWI/SNF complex. *EMBO J*. 2014;33(20):2332-2348.

47. Wang D, Paz-Priel I, Friedman AD. NF-kappa B p50 regulates C/EBP alpha expression and inflammatory cytokine-induced neutrophil production. *J Immunol*. 2009;182(9):5757-5762.